Robotics and Computer-Integrated Manufacturing 31 (2015) 40–50

Contents lists available at ScienceDirect

Robotics and Computer-Integrated Manufacturing

journal homepage: www.elsevier.com/locate/rcim

Inverse kinematics and rigid-body dynamics for a three rotational degrees of freedom parallel manipulator

Yongjie Zhao *, Ke Qiu, Shuangxi Wang, Ziqiang Zhang

Department of Mechatronics Engineering, Shantou University, Shantou, Guangdong 515063, PR China

ARTICLE INFO

Article history:
Received 25 September 2013
Received in revised form
14 July 2014
Accepted 14 July 2014

Keywords:
Parallel manipulator
Singularity
Jerk
Torque
Power
Energy consumption

ABSTRACT

Modeling and analysis of inverse kinematics and rigid-body dynamics for a three rotational degrees of freedom (DOF) parallel manipulator are conducted in this research. In the inverse kinematics model, the position, velocity, acceleration, jerk and singularity are considered. The rigid-body dynamic model is developed based on the principle of virtual work and the concept of link Jacobian matrices. In this research, the inverse dynamic analysis of the parallel manipulator is carried out in an exhaustive decoupled way. The total actuating torques, the torques related to the acceleration, velocity, and gravity, the torques related to the moving platform, strut, slider, lead screw, and motor rotor-coupler, and the torques related to external forces are calculated. The total actuating powers, the powers related to the acceleration component of torque, velocity component of torque, gravity component of torque, and the powers related to the moving platform, strut, slider, lead screw, and motor rotor-coupler are also achieved. For the pre-defined trajectory, the required output work for the *i*-th driving motor is obtained through numerical integration technique. Simulation is conducted to obtain the positions, velocities, accelerations, jerks, torques, powers, and energy consumptions.

1. Introduction

The rotary tables are widely used in manufacturing tools such as the CNC machining centers [1–5]. The existing rotary tables are usually built using serial manipulators. In order to enhance the load capability, parallel manipulators with rotational degrees of freedom have been used in the development of the rotary tables [6–9]. Compared with the general 6-DOF parallel manipulators, low mobility parallel manipulators with less degrees of freedom have simpler mechanical structures and fewer actuators, thus being able to be built with low manufacturing costs and simple control mechanisms. Compared with the serial structure manipulators, low mobility parallel manipulators can provide improved rigidity, reconfigurability, and static balance. Because of these reasons, research on low mobility parallel manipulators has attracted much interest from academic and industrial communities [10]. Due to the high working load requirement, the inverse kinematics and rigid-body dynamics should be considered in the design of rotary tables using the low mobility parallel manipulators.

The inverse kinematics can be used for optimal design of a mechanism. The rigid-body dynamic characteristic should be investigated when the parallel manipulator is used with high acceleration situation, high speed operation and/or high load application [11]. Many research works have been conducted on the rigid-body dynamics of the parallel manipulators [11–21]. Several approaches such as the Newton–Euler method [12], the Lagrangian method [13], the Kane's method [14], and the virtual work principle [15–24] have been selected to model and analysis of the dynamics of the parallel manipulators. The total actuating torques and powers can be decomposed into different components related to the acceleration, velocity, gravity, and external force. They can also be decoupled into the components related to the moving platform, strut, slider, lead screw, motor rotor-coupler, and external force [16]. The rigid-body dynamic model has been used for the performance evaluation [15,25], dynamic optimum design [11,26–27], computed-torque control [28], and servomotor selection [29]. The existing methods for inverse kinematics and rigid-body dynamics of the parallel manipulators seldom considers the jerk [30–31], power [15,25,29,32], and energy consumption [17,32]. In fact, the impacts of jerk [31] and energy efficiency [11,17,33] should also be considered in the design of the parallel manipulators.

The objective of the research presented in this paper aims at developing the analysis models for inverse kinematics and

* Corresponding author.
E-mail addresses: meyjzhao@stu.edu.cn (Y. Zhao), mekeqiu@163.com (K. Qiu), sxwang@stu.edu.cn (S. Wang), zqzhang@stu.edu.cn (Z. Zhang).

http://dx.doi.org/10.1016/j.rcim.2014.07.002
0736-5845/

rigid-body dynamics of a three rotational degrees of freedom parallel manipulator considering the position, velocity, acceleration, jerk, singularity, torque, power, and energy consumption. The paper is organized as follows. The three rotational degrees of freedom parallel manipulator is explained in Section 2. The inverse kinematics considering the position, velocity, acceleration, jerk and singularity are provided in Section 3. Inverse rigid-body dynamics considering the power and energy consumption is investigated in Section 4. Simulations and conclusions are given in Sections 5 and 6.

2. A three rotational degrees of freedom parallel manipulator

The parallel manipulator is shown in Figs. 1 and 2. This parallel manipulator is composed of a moving platform connected with the base platform through four kinematic chains. The central kinematic chain is fixed on the base platform at one end and connected to the moving platform using a revolute joint and a universal joint at the other end. The three outer kinematic chains connect the moving platform and the three sliders using spherical joints and struts with fixed-length. Each slider is driven by a DC motor via a lead screw. Due to the proper constraints of the central kinematic chain, the manipulator has three rotational degrees of freedom.

As shown in Figs. 2 and 3, the following coordinate systems are defined for the modeling of the rigid-body dynamics: the reference coordinate system $O-xyz$ is attached to the center of the base platform, and the moving coordinate system $O'-uvw$ is located at the center of mass of the moving platform. The orientation of the moving platform can be described by a rotation matrix ${}^{O}\mathbf{R}_{O'}$. Let the rotation matrix be defined by the parameters of roll, pitch, and yaw angle, namely, a rotation of ϕ_x about the fixed x-axis, followed by a rotation ϕ_y about the fixed y-axis, and a rotation ϕ_z about the fixed z-axis. Thus, the rotation matrix can be obtained by

$$ {}^{o}\boldsymbol{R}_{o'} = \mathrm{Rot}(z, \phi_z)\mathrm{Rot}(y, \phi_y)\mathrm{Rot}(x, \phi_x) \tag{1} $$

The angular velocity of the moving platform is given by [24]

$$ \boldsymbol{\omega} = [\dot{\phi}_x \quad \dot{\phi}_y \quad \dot{\phi}_z]^T \tag{2} $$

The orientation of each kinematic strut with respect to the fixed base can be described by two Euler angles. As shown in Fig. 4, the local coordinate system of the i-th strut can be thought of as a rotation of ϕ_i about the z-axis resulting in a $C_i-x_i'y_i'z_i'$ system followed by another rotation of φ_i about the rotated y_i'-axis. So the rotation matrix of the i-th strut can be written as

$$ {}^{o}\boldsymbol{R}_i = \mathrm{Rot}(z, \phi_i)\mathrm{Rot}(y_i', \varphi_i) = \begin{bmatrix} c\phi_i c\varphi_i & -s\phi_i & c\phi_i s\varphi_i \\ s\phi_i c\varphi_i & c\phi_i & s\phi_i s\varphi_i \\ -s\varphi_i & 0 & c\varphi_i \end{bmatrix} \tag{3} $$

The unit vector along the lead screw in the coordinate system$O-xyz$is

$$ \boldsymbol{w}_i = {}^{o}\boldsymbol{R}_i {}^{i}\boldsymbol{w}_i = {}^{o}\boldsymbol{R}_i \begin{bmatrix} 0 \\ 0 \\ 1 \end{bmatrix} = \begin{bmatrix} c\phi_i s\varphi_i \\ s\phi_i s\varphi_i \\ c\varphi_i \end{bmatrix} \tag{4} $$

So the Euler angles ϕ_i and φ_i can be computed as follows:

$$ \begin{cases} c\varphi_i = \boldsymbol{w}_{iz} \\ s\varphi_i = \sqrt{\boldsymbol{w}_{ix}^2 + \boldsymbol{w}_{iy}^2}, \quad (0 \le \varphi_i < \pi) \\ s\phi_i = \boldsymbol{w}_{iy}/s\varphi_i \\ c\phi_i = \boldsymbol{w}_{ix}/s\varphi_i \\ \text{if} \varphi_i = 0, \text{then } \ \phi_i = 0 \end{cases} \tag{5} $$

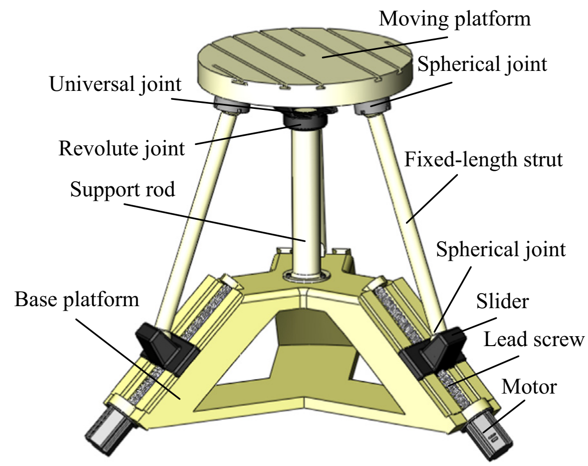

Fig. 1. The three rotational degrees of freedom parallel manipulator.

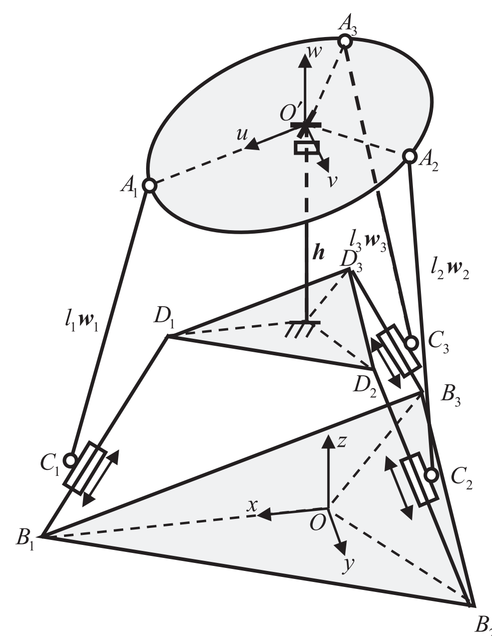

Fig. 2. Schematic diagram of the parallel manipulator.

3. Inverse kinematics

3.1. Position analysis

As shown in Fig. 3, the position equation associated with the i-th kinematic chain can be written as

$$ \boldsymbol{h} + \boldsymbol{r}_{ai} = l_i\boldsymbol{w}_i + \boldsymbol{r}_{bi} + \boldsymbol{d}_i + q_i\boldsymbol{e}_i \tag{6} $$

where $\boldsymbol{h}$, q_i, $\boldsymbol{e}_i$, l_i, $\boldsymbol{w}_i$, $\boldsymbol{r}_{ai}$, $\boldsymbol{r}_{bi}$, and $\boldsymbol{d}_i$ denote the position vector OO', the joint variable, the unit vector along the lead screw B_iD_i, the length of the strut C_iA_i, the unit vector along the strut C_iA_i, the vector $O'A_i$, the vector OB_i, and the vector from the center of the point of the joint C_i to the lead screw, respectively.

3.2. Velocity analysis

Taking the derivative of Eq. (6) with respect to time, we can obtain:

$$ \boldsymbol{\omega} \times \boldsymbol{r}_{ai} = \dot{q}_i\boldsymbol{e}_i + \boldsymbol{\omega}_i \times l_i\boldsymbol{w}_i \tag{7} $$